

$B_s^0 \rightarrow \mu^+ \mu^-$ IN LHCb

© 2009 D. Martinez Santos*
(on behalf of the LHCb Collaboration)

Universidade de Santiago de Compostela, Spain

Received September 18, 2008; in final form, February 12, 2009

Due to its sensitivity to New Physics contributions, the branching ratio of the very rare decay $B_s^0 \rightarrow \mu^+ \mu^-$ is one of the most interesting measurements using the first data from the LHC accelerator. The analysis strategy for the study of this channel in the LHCb experiment is presented, as well as a review of the potential of the experiment in such study, using the latest simulations. With four months of nominal data taking, any enhancement from the Standard Model prediction can be excluded.

PACS: 12.15.Mm, 13.20.He

1. INTRODUCTION AND MOTIVATION

Precision observables at low energy allow to access information at higher energy scales, constraining possible New Physics (NP) scenarios. That is the case of $b \rightarrow s\gamma$ transitions [1, 2] or the muon anomalous dipole moment [3, 4]. The branching ratio $\text{BR}(B_s^0 \rightarrow \mu^+ \mu^-)$ has been identified as a very interesting potential constraint on the parameter space of NP models [5]. The SM prediction is $\text{BR}(B_s^0 \rightarrow \mu^+ \mu^-) = (3.35 \pm 0.32) \times 10^{-9}$ [6], while the current upper limit given by Tevatron is $\text{BR}(B_s^0 \rightarrow \mu^+ \mu^-) < 47 \times 10^{-9}$ at 90% C.L. [7]. Hence, NP can contribute up to one order of magnitude. A special set of NP models, where this measurement has important implications, are Supersymmetric (SUSY) models, such as Minimal Supersymmetric Standard Model (MSSM) [8]. In these models, $\text{BR}(B_s^0 \rightarrow \mu^+ \mu^-)$ increases with the sixth power of the ratio of u -type and d -type Higgs vacuum expectation values [9], $\tan\beta$. For SUSY with low $\tan\beta$, $\text{BR}(B_s^0 \rightarrow \mu^+ \mu^-)$ can be as small as in the SM and, in fact, models with extra phases of CP violation may predict values even lower than the SM [10]. This article explains how the data analysis for the extraction of such BR (Section 2) is planned to be done in LHCb, following the approach shown in [11] but modified in order to minimize the dependence on simulation, making use of control channels. In Section 3, simulation of signal and background is used to extract the potential of the LHCb in the measurement/exclusion of $\text{BR}(B_s^0 \rightarrow \mu^+ \mu^-)$. Finally, in Section 4, different possible experimental results are interpreted in the framework of MSSM.

2. ANALYSIS STRATEGY

The data analysis for extracting $\text{BR}(B_s^0 \rightarrow \mu^+ \mu^-)$ can be schematized as follows:

1. Reconstruction of all $\mu^+ \mu^-$ combinations¹⁾ on triggered²⁾ events. A given particle is considered as a μ candidate if it has a minimum number of associated hits in the Muon System, depending on its momentum (see “isMuon” definition [12]).

2. Selection of $B_s^0 \rightarrow \mu^+ \mu^-$ candidates according to event properties. This step is needed in order to remove a large amount of background, hence reducing by several orders of magnitude the size of the data sample, and has been modified since [11]. Section 2.1 describes how it is done.

3. Classification of each selected event in a binned 3D phase space, according to the following properties. Geometry Likelihood (GL): takes into account the geometrical properties of the candidate (it is explained in more detail in Section 2.2). Particle Identification (PID) likelihood: it is the combined probability of the muon candidates to be real muons, over all the other particle hypothesis. Invariant mass of the $\mu^+ \mu^-$ couple: only events in a window of ± 60 MeV ($\approx 3\sigma$) around B_s^0 peak (5369.6 MeV) are considered.

4. The number of background events is computed interpolating from the mass sidebands (events outside the ± 60 MeV window), where no signal is present.

¹⁾Current Monte Carlo simulations show that the probability, for a $B_s^0 \rightarrow \mu^+ \mu^-$ decay produced in the LHCb interaction point, to be reconstructed as a $\mu^+ \mu^-$ candidate is $\approx 10\%$. Here the main effect is the geometrical acceptance of the LHCb detector.

²⁾The LHCb trigger is highly efficient ($\approx 85\%$) for $B_s^0 \rightarrow \mu^+ \mu^-$ reconstructed decays.

*E-mail: diego.martinez.santos@cern.ch

5. The probability for a signal event to fall in each bin of the phase space is determined. Several control channels are used for that: for the geometrical properties and the invariant mass, the two-body decays of B_d^0 and B_s^0 , here abbreviated as $B \rightarrow h^+ h'^-$ (where $h = K, \pi, h' = K, \pi$), are used. Section 2.3 describes this subject in more detail. For PID properties the control channels are: calibration muons (such as MIPs in the calorimeter, prompt $J/\psi \rightarrow \mu^+ \mu^-$ decays or $B \rightarrow J/\psi(\mu\mu)X$), and hadrons coming from decays of prompt $K_s^0, \Lambda \rightarrow p\pi$ and $D^* \rightarrow D^0(K\pi)\pi$. The momentum range of signal particles is known from $B \rightarrow h^+ h'^-$, thus the appropriate kinematical region from those PID control channels can be chosen.

6. Normalization: in order to translate the number of signal events into a branching ratio, a measurement of the number of events from a decay with a known BR is needed. Then $\text{BR}(B_s^0 \rightarrow \mu^+ \mu^-)$ can be extracted from

$$\begin{aligned} \text{BR}(B_s^0 \rightarrow \mu^+ \mu^-) &= \\ &= \frac{\text{BR}_n \cdot \epsilon_n^{\text{REC}} \epsilon_n^{\text{SEL/REC}} \epsilon_n^{\text{TRIG/SEL}} \frac{f_n}{f_{B_s^0}} \frac{N}{N_n}}{\epsilon^{\text{REC}} \epsilon^{\text{SEL/REC}} \epsilon^{\text{TRIG/SEL}}} \end{aligned}$$

Here, the quantities with n subscript refer to normalization channel. N is the number of events, ϵ are the efficiencies of different parts of the process (reconstruction, selection, and trigger), and f the hadronization fractions of b quark is the probability to hadronize in the different hadrons.

7. The statistical method [13] is used, in the case of exclusion, to get the maximum number of signal events compatible with the observed data configuration. In case of observation, it is used to get the significance.

As there is no accurate measurement of any B_s^0 branching ratio, normalization to B^+ or B_d^0 decays is preferred. However, this implies a systematic error of 14% coming from the ratio $f_n/f_{B_s^0}$ [14]. The normalization channel chosen is the decay $B^+ \rightarrow J/\psi(\mu^+ \mu^-)K^+$ because of its large statistics and the J/ψ muons, which correlate the reconstruction and trigger efficiencies for both signal and normalization channels.

2.1. Event Selection

The $B_s^0 \rightarrow \mu^+ \mu^-$ event selection is designed to be the same, apart from MuonID requirement, as for the two-body B decays used for GL calibration. It avoids any selection bias in the distribution of the GL. Because of the large pion and kaon combinatorial in the LHC, a selection as soft as in [11] is not suitable for those control channels. The new selection used

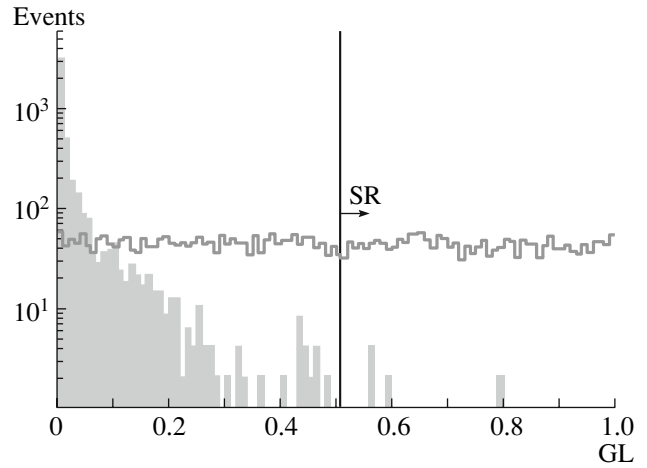


Fig. 1. Distribution of the discriminant variable GL. Grey filled histogram is for $b\bar{b} \rightarrow \mu\mu X$, non-filled histogram is for $B_s^0 \rightarrow \mu^+ \mu^-$. The normalization of both components is arbitrary. The sensitive region (SR) is defined as $GL > 0.5$.

adds to [11] the displacement of the Secondary Vertex with respect to the Primary Vertex ($>12\sigma$), the transverse momentum of the B meson (>700 MeV), and the impact parameter significance (IPS) of the tracks (h^+, h'^- or μ^+, μ^-) to the PV ($>3.5\sigma$). Furthermore, a similar selection for $B^+ \rightarrow J/\psi K^+$ candidates has the advantage that the fraction of selection efficiencies in the normalization is less sensitive to systematic uncertainties. Properties of B mesons are used in such selection, while the two-track vertex properties are accounted using the $J/\psi \rightarrow \mu\mu$ vertex. The cut on the IPS of the muons used for $B_s^0 \rightarrow \mu^+ \mu^-$ is applied on the kaon of $B^+ \rightarrow J/\psi K^+$. Because of the tight cut on the displacement of the decay vertex, the efficiency of that IPS cut becomes the same for signal and normalization channel. In order to reject

Event yields in SR per nominal year (2 fb^{-1}) ($b\bar{b} \rightarrow \mu\mu X$ category does not include any of the other modes presented in the table, $B_s^0 \rightarrow \mu^+ \mu^- \gamma$ does not include $B_s^0 \rightarrow \mu^+ \mu^-$ with final-state radiation, because it is already included in $B_s^0 \rightarrow \mu^+ \mu^-$)

Source	Events in SR per nominal year
$B_s^0 \rightarrow \mu^+ \mu^-$	22.8
$b\bar{b} \rightarrow \mu\mu X$	150 (<324 at 90% C.L.)
$B \rightarrow h^+ h^-$	8 (<17.2 at 90% C.L.)
$B_s^0 \rightarrow \mu^+ \mu^- \gamma$	0 (<2.44 at 90% C.L.)
$B_c^+ \rightarrow J/\psi(\mu^+ \mu^-)\mu^+ \nu_\mu$	0 (<20 at 90% C.L.)

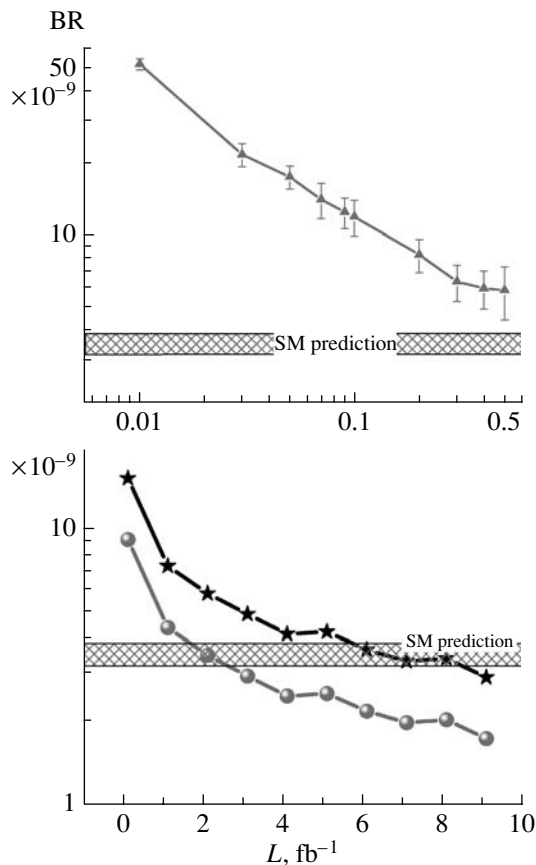


Fig. 2. (Top) $\text{BR}(B_s^0 \rightarrow \mu^+ \mu^-)$ excluded at 90% C.L. as a function of the integrated luminosity L if no signal is present. (Bottom) Luminosity needed for the observation of a certain BR at (circles) 3σ and (stars) 5σ level.

a large amount of combinatorial muons, a cut on the J/ψ invariant mass window is needed in the selection of $B^+ \rightarrow J/\psi K^+$. However, due to the large J/ψ statistics, the efficiency of such cut is expected to be well known.

2.2. Geometry Likelihood

The GL is built with Monte Carlo (MC) samples of signal and background and returns, for a given event, a χ_s^2 of the signal hypothesis and a χ_b^2 of the background hypothesis. The quantity $\chi_b^2 - \chi_s^2$, after a mathematical transformation that makes the distribution to be flat for signal, is used as discriminant variable. Its distribution for signal and background is shown in Fig. 1. The input variables used and the mathematical procedure to extract the χ^2 are described in [11].

The GL is the most discriminant variable used in the 3D phase space, and almost all the sensitivity is accumulated in the region of $\text{GL} > 0.5$, called for this reason “sensitive region” (SR).

2.3. Calibration of Signal Properties

Because real-data properties may differ from MC simulation, the distribution of the GL needs to be extracted from data³⁾. For the background it is computed from the sidebands. For the signal the two-body B decays are used, because they have the same geometrical and kinematical properties as $B_s^0 \rightarrow \mu^+ \mu^-$. Large statistics is expected from these channels, as well as high purity in the interesting phase-space regions. The main issue for GL calibration is to avoid the bias coming from the hard cuts of hadronic trigger, but in principle it can be done by using only those $B \rightarrow h^+ h'^-$ events triggered independently of the signal (TIS)⁴⁾, where no information from the $B \rightarrow h^+ h'^-$ decay is needed for the event to trigger. Although this procedure implies a strong reduction on statistics of the calibration channel, several hundreds (few thousands) of TIS $B \rightarrow h^+ h'^-$ are expected in 0.1 (0.5) fb^{-1} , which are enough to not to be the main source of uncertainty.

The invariant-mass distribution for $B_s^0 \rightarrow \mu^+ \mu^-$ is also extracted from $B \rightarrow h^+ h'^-$, in particular, from $B_s^0 \rightarrow K^+ K^-$. The excellent performance of RICH detectors allows to separate that component from the other two-body B decays with a reasonable purity. Then the σ of the distribution can be known with a precision of $\approx 3\%$ already with 0.1 fb^{-1} of integrated luminosity.

3. POTENTIAL OF THE EXPERIMENT

3.1. Event Yields

The main sources of background for the LHCb experiment are assumed to come from inclusive $b\bar{b}$ events. This is confirmed by the fact that after the LHCb muon trigger, running on a minimum bias sample, most of the events left are $b\bar{b}$. The analysis of a full MC simulation sample of those events, corresponding to $\approx 0.08 \text{ pb}^{-1}$, shows that the main contribution for $B_s^0 \rightarrow \mu^+ \mu^-$ are inclusive $b\bar{b} \rightarrow \mu\mu X$ events, with a fraction increasing rapidly to $\approx 100\%$ when the GL increases. A 5.3-pb⁻¹ MC sample of $b\bar{b} \rightarrow \mu\mu X$ was then used in order to estimate the background level for $B_s^0 \rightarrow \mu^+ \mu^-$ studies. This background is expected to contribute with $\approx 80 \text{ K}$ events in 2 fb^{-1} (the expected integrated luminosity in one nominal year), but only 150 of them fall in the SR.

³⁾Also, the real data can be used to redefine the GL, but this point is not discussed here.

⁴⁾This category does not exclude the possibility to trigger on the signal. In this case there are two different ways to trigger in the same event. For this reason, no trigger bias is expected in the TIS category.

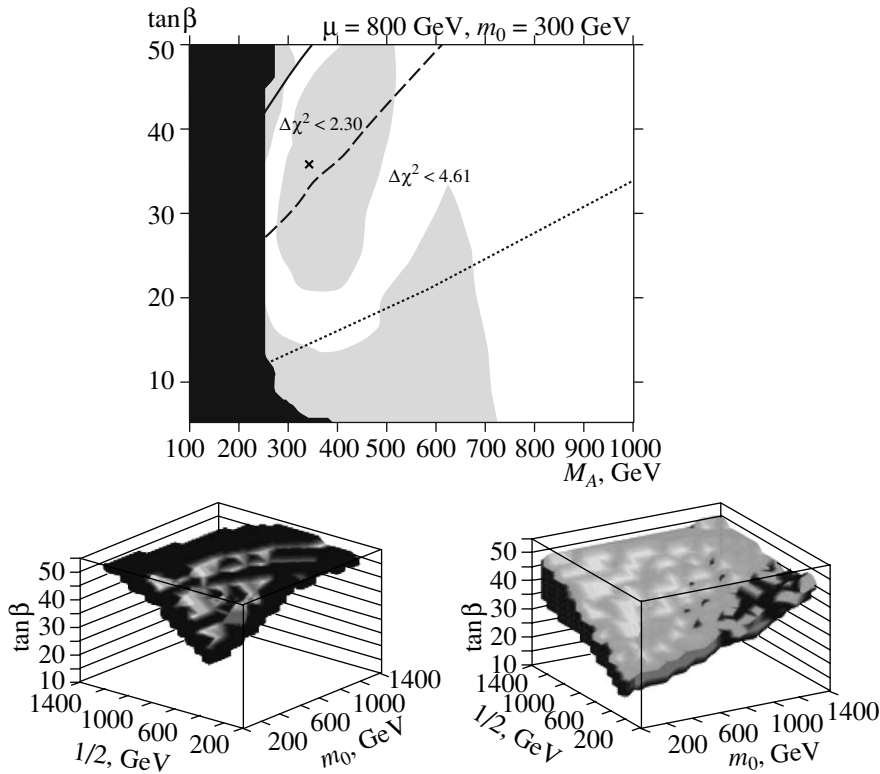


Fig. 3. Different SUSY constraints depending on the experimental results. (Top) NUHM benchmark plot $\tan\beta$ vs. M_A . The cross is the best minimum of the fit. The lines are regions compatible with different values of $\text{BR}(B_s^0 \rightarrow \mu^+ \mu^-)$: 10^{-7} (solid line), 2×10^{-8} (dashed line), and 5×10^{-9} (dotted line). (Bottom) Regions of CMSSM parameter space compatible with different measurements of $\text{BR}(B_s^0 \rightarrow \mu^+ \mu^-)$: (left) 10^{-8} with 5σ , (right) 5×10^{-9} with 3σ , for $\mu > 0$ and $A_0 = 0$.

Several other specific backgrounds were analyzed as well. The expected yields are summarized in the table.

For $B_s^0 \rightarrow \mu^+ \mu^-$, the expected annual yield is $\approx 46 \frac{\text{BR}(B_s^0 \rightarrow \mu^+ \mu^-)}{\text{BR}(B_s^0 \rightarrow \mu^+ \mu^-)_{\text{SM}}}$ reconstructed, selected, and triggered events. Due to the flat distribution of the GL, in the SR the yield $\approx 23 \frac{\text{BR}(B_s^0 \rightarrow \mu^+ \mu^-)}{\text{BR}(B_s^0 \rightarrow \mu^+ \mu^-)_{\text{SM}}}$ is expected.

3.2. Exclusion/Measurement Potential

From the MC predictions of signal and background properties and annual yields, the potential of the LHCb experiment on the exclusion or measurement of $\text{BR}(B_s^0 \rightarrow \mu^+ \mu^-)$ can be extracted. Figure 2 (top) shows the BR excluded at 90% C.L. as a function of the integrated luminosity, up to 0.5 fb^{-1} (one quarter of nominal data-taking year). The expected limit at the end of Tevatron, 2×10^{-8} , is overtaken with less than 0.1 fb^{-1} . With 0.5 fb^{-1} limits on the BR down to SM prediction are set if no signal is present.

In the case of presence of signal, the luminosity needed for the 3σ observation of a given BR is shown on Fig. 2 (bottom). Between 2 and 5 fb^{-1} is enough for a 3σ observation if the BR is the SM prediction.

4. EXAMPLES OF IMPLICATIONS

CMSSM (constrained MSSM) is commonly used to show the potential of experimental measurements on SUSY searches, because it has only five free parameters. This model is used in Section 4.2 to show how the value of the measured branching ratio constrains the values of SUSY parameters. For the case of exclusion (Section 4.1) a more general approach, called Non-Universal Higgs Masses (NUHM) [15, 16], is used in order to show the luminosity needed to exclude the current best χ^2 of its parameter fit.

4.1. Exclusion of the Best χ^2 of Non-Universal Higgs Masses

NUHM reduces the MSSM parameter phase space in almost the same way as CMSSM, but avoiding the condition of universal Higgs masses, providing a framework for the study of the Higgs sector. Relaxing such condition lets the parameters M_A and $|\mu|$ to be free. The parameter M_A is the mass of the physical CP -odd neutral Higgs A^0 .

If no signal is observed, LHCb accesses the region of the minimum of the SUSY fit with very low

integrated luminosity (see Fig. 3, top), $\approx 0.1 \text{ fb}^{-1}$ is needed to exclude the best χ^2 point and 0.5 fb^{-1} to exclude all the region (in M_A vs. $\tan\beta$ plane) with $\Delta\chi^2 < 2.3$ around it. For the other three benchmark surfaces in [16] the situation is similar.

4.2. Observation and CMSSM

The main CMSSM parameters which affect $\text{BR}(B_s^0 \rightarrow \mu^+\mu^-)$ are $\tan\beta$, m_0 , and $m_{1/2}$. For the study shown in this section, the other two parameters were fixed to $A_0 = 0$ and $\mu > 0$. The programs SoftSUSY⁵⁾ and SUITY v-1.0⁶⁾ were used to compute the surfaces in the $\tan\beta$, m_0 , and $m_{1/2}$ compatible with a given $\text{BR}(B_s^0 \rightarrow \mu^+\mu^-)$ and with the experimental constraints $M_{h^0} > 114 \text{ GeV}$ (lightest Higgs mass) and $M_W = 80.398 \pm 0.025 \text{ GeV}$.

Large values of $\text{BR}(B_s^0 \rightarrow \mu^+\mu^-)$, such as 1×10^{-8} , can be measured with very low integrated luminosities. The parameter space surface compatible with a 5σ discovery of $\text{BR}(B_s^0 \rightarrow \mu^+\mu^-) = 1 \times 10^{-8}$ is shown in Fig. 3 (bottom, left). Of course, values just slightly larger than SM predictions need more integrated luminosity to be measured. The implications of a 3σ observation of $\text{BR}(B_s^0 \rightarrow \mu^+\mu^-) = 5 \times 10^{-9}$ are shown in Fig. 3 (bottom, right).

I would like to thank J.A. Hernando, F. Teubert, E. Lopez Asamar, A. Camboni, R. Louvot, H. Ruiz, and G. Lanfranchi, from the LHCb Collaboration, for their work included here and the organizers of the XXXVI ITEP Winter School for their good organization and hospitality. I also thank the financial support provided by Programa Nacional de Becas FPU (MEC).

REFERENCES

1. S. Chen *et al.* (CLEO Collab.), Phys. Rev. Lett. **87**, 251807 (2001); P. Koppenburg *et al.* (BELLE Collab.), Phys. Rev. Lett. **93**, 061803 (2004); B. Aubert *et al.* (BABAR Collab.), hep-ex/0207076.
2. T. Hurth, Rev. Mod. Phys. **75**, 1159 (2003).
3. G. W. Bennett *et al.* (Muon g-2 Collab.), Phys. Rev. Lett. **92**, 161802 (2004).
4. M. Davier, S. Eidelman, A. Hocker, and Z. Zhang, Eur. Phys. J. C **31**, 503 (2003); M. Davier, hep-ph/0701163v2.
5. A. Dedes, H. K. Dreiner, and U. Nierste, Phys. Rev. Lett. **87**, 251804 (2001); C. S. Huang, W. Liao, Q. S. Yan, and S. H. Zhu, Phys. Rev. D **63**, 114021 (2001).
6. M. Blanke *et al.*, TUM-HEP-626/06; JHEP **0610**, 003 (2006); hep-ph/0604057v5.
7. CDF Collab., CDF Public Note 8956.
8. S. P. Martin, hep-ph/9709356.
9. S. R. Choudhury and N. Gaur, Phys. Lett. B **451**, 86 (1999); P. H. Chankowski and L. Slawianowska, Phys. Rev. D **63**, 054012 (2001); K. S. Babu and C. F. Kolda, Phys. Rev. Lett. **84**, 228 (2000); C. Bobeth, T. Ewerth, F. Kruger, and J. Urban, Phys. Rev. D **64**, 070414 (2001).
10. J. Ellis *et al.*, CERN-PH-TH/2007-136; arXiv: 0708. 2079v1 [hep-ph].
11. D. Martinez Santos, J. A. Hernando, and F. Teubert, CERN-LHCb-2007-033.
12. E. Polycarpo and M. Gandelman, LHCb 2005-099.
13. A. L. Read, CERN Yellow Report 2000-005.
14. W.-M. Yao *et al.*, J. Phys. G **33**, 1 (2006).
15. J. Ellis *et al.*, CERN-PH-TH/2007-138; arXiv: 0709. 0098v1 [hep-ph].
16. J. Ellis *et al.*, CERN-TH/2002-81; hep-ph/0204192.

⁵⁾Provided by Ben Allanach (Cambridge).

⁶⁾Provided by Athanasios Dedes (Durham).